UHASSELT
KNOWLEDGE IN ACTION

Maastricht University

Faculty of Medicine and Life Sciences
School for Life Sciences
Master of Biomedical Sciences

Master's thesis

Pressing the reset button: Enhancing remyelination in MS through phagocyte metabolic reprogramming

Seçilay Bayin

Thesis presented in fulfillment of the requirements for the degree of Master of Biomedical Sciences, specialization Molecular Mechanisms in Health and Disease

SUPERVISOR :

Prof. dr. Jerome HENDRIKS

MENTOR :

dr. Sanne VERBERK

2025
2026

Transnational University Limburg is a unique collaboration of two universities in two countries: the University of Hasselt and Maastricht University.

UHASSELT
KNOWLEDGE IN ACTION

www.uhasselt.be
Universiteit Hasselt
Campus Hasselt:
Martelarenlaan 42 | 3500 Hasselt
Campus Diepenbeek:
Agoralaan Gebouw D | 3590 Diepenbeek

UHASSELT
KNOWLEDGE IN ACTION

Maastricht University

Faculty of Medicine and Life Sciences
School for Life Sciences
Master of Biomedical Sciences

Master's thesis

Pressing the reset button: Enhancing remyelination in MS through phagocyte metabolic reprogramming

Seçilay Bayin

Thesis presented in fulfillment of the requirements for the degree of Master of Biomedical Sciences, specialization Molecular Mechanisms in Health and Disease

SUPERVISOR :

Prof. dr. Jerome HENDRIKS

MENTOR :

dr. Sanne VERBERK

Pressing the reset button: Enhancing remyelination in MS through phagocyte metabolic reprogramming

Seçilay Bayin[1], Dr. Sanne Verberk[2], Prof. Dr. Jerome Hendriks[2]

[1]Department of Medicine and Life Sciences, University Hasselt, Campus Diepenbeek, Agoralaan Building D 3590 Diepenbeek, Belgium.

2

[2]Department of Immunology and Infection, Biomedical Research Institute (BIOMED), Hasselt University, Agoralaan Gebouw C 3590 Diepenbeek, Belgium.

*Running title: *Phagocyte metabolic reprogramming to boost repair*

To whom correspondence should be addressed: Prof. Dr. Jerome Hendriks, Tel: +32 (11) 26 92 07; Email: Jerome.Hendriks@uhasselt.be

Keywords: Multiple Sclerosis, Microglia, Metabolic Reprogramming, Lipid Handling, Remyelination

ABSTRACT

Multiple sclerosis (MS) is a chronic neurodegenerative disease affecting the central nervous system, characterized by neuroinflammation and demyelination, which disrupt signal transmission between neurons. There is currently no cure, current treatments focus on managing acute attacks and alleviating symptoms. MS pathology features multifocal lesions, primarily in white matter, that transition from active to smoldering as the disease progresses, with an active rim of macrophages and microglia both reparative and damaging phenotypes. These cells become overloaded with myelin debris, resulting in foamy, dysfunctional phagocytes. Studying metabolic changes in foamy phagocytes may uncover therapeutic targets, as their metabolism is linked to their phenotype. Pro-inflammatory macrophages primarily use glycolysis, while anti-inflammatory cells favor oxidative phosphorylation (OXPHOS). This study aims to elucidate the metabolic changes in myelin-treated bone marrow-derived macrophages (BMDMs) and to reprogram their metabolism by inhibiting glycolysis with the GLUT1 inhibitor BAY-876, along with siRNAs targeting GLUT1 and hexokinase 2 (HK2). Extracellular flux analysis revealed that the inhibition of glycolysis reduced the inflammatory response of myelin-laden BMDMs, with decreased NO production and lowered expression of inflammatory genes. However, this approach was not able to reprogram the metabolism towards increased OXPHOS. Additionally, an improvement in lipid load was not observed. While these results highlight the potential of metabolic reprogramming in myelin-loaded phagocytes to enhance their function, optimization is necessary to fully realize this therapeutic potential, thereby possibly improving lipid load and promoting remyelination. This novel approach holds promise for advancing treatments for progressive MS, while simultaneously advancing therapeutic avenues for other neurodegenerative disorders.

INTRODUCTION

Globally, approximately 2.8 million people are affected by multiple sclerosis (MS), a chronic neurodegenerative disease of the central nervous system (CNS) (1). The onset of MS is characterized by acute, multifocal inflammation primarily localized in the white matter of the CNS, which attracts macrophages and microglia to the affected area, targeting the myelin sheaths surrounding axons (2). This immune response leads to demyelination and axonal degeneration, resulting in the formation of multiple glial scars within the CNS. The lesions that develop disrupt signal transmission between neurons, leading to a variety of symptoms, including muscle weakness, fatigue, and vision impairments, which can vary based on the lesion's location and severity (3). Currently, treatment of MS primarily focus on managing acute attacks, by suppressing the activated immune response, and alleviating symptoms. However, a complete cure remains elusive (4). In MS, various types of lesions develop, with certain types being more prevalent at specific stages of the disease. In the

early stages, most frequently identified as relapsing-remitting MS (RRMS), the majority of lesions are active, resulting from inflammation and microglial activity. Over time, most of these active lesions become inactive, while some show partial remyelination, or in the case of progressive MS, transition into smoldering lesions. These smoldering lesions are not prone to remyelination, but instead persist and gradually enlarge over time (5, 6). Smoldering lesions are characterized by an inactive central core surrounded by a peripheral zone composed of macrophages and microglia (5). These cells exhibit diverse phenotypic states that together form an active, slowly expanding rim sustained by chronic low-grade inflammation. A portion of the microglia population present in these lesions exhibits a reparative phenotype, characterized by efficient clearance of myelin debris, a high capacity for cholesterol efflux, and anti-inflammatory properties (7, 8). However, the predominant cells in these areas are damaging foamy microglia (7, 9) . These cells are overloaded with myelin debris, which impairs their function and hinders their ability to revert to a reparative state. Foamy microglia display reduced phagocytic activity, deficits in lipid processing, efflux, and lipophagy, along with sustained inflammation. This dysfunction contributes to the expansion of smoldering lesions and ultimately leads to the failure of remyelination (10).

The mechanisms that allow microglia to switch between pro-inflammatory and anti-inflammatory phenotypes during myelin damage and repair in multiple sclerosis, and why these mechanisms fail in smoldering lesions, remain unclear (7). For example, various studies have produced conflicting results regarding the short-term myelin exposure of microglia. While most suggest that this exposure induces a disease-promoting phenotype, some studies challenge this idea, observing no changes or even a shift towards a pro-remyelination state upon myelin uptake (6, 11). Conversely, long-term exposure to myelin appears to skew these cells towards promoting lesion progression (10, 12). Differences in metabolic activity can significantly influence how macrophages contribute to disease progression. For instance, pro-inflammatory macrophages tend to favor the glycolytic pathway, which provides a rapid energy supply to support acute inflammatory responses. In the context of MS, this metabolic preference results in the release of inflammatory cytokines, thereby contributing to the worsening of MS lesions (6, 7, 13). In contrast, enhanced oxidative phosphorylation and fatty acid oxidation (FAO) are associated with an anti-inflammatory and pro-reparative phenotype (13).

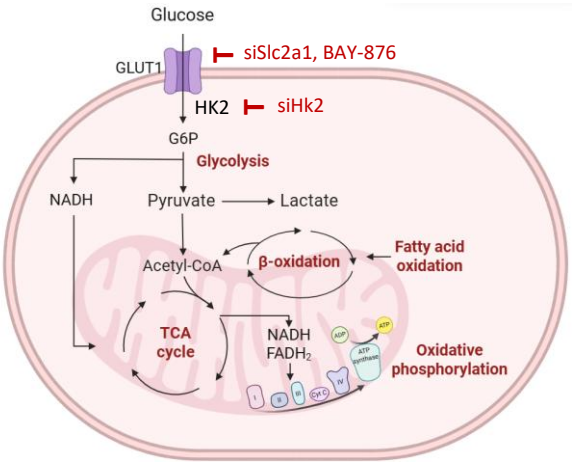

Fig. 1 – Schematic overview of major cellular metabolic pathways. Glycolysis converts glucose, which enters the cell via GLUT1, into G6P using HK2, and then into pyruvate. β-oxidation breaks down long-chain fatty acids into acetyl-CoA, with both pathways generating ATP and reducing equivalents (NADH and $FADH_2$). These reducing equivalents supply electrons to the ETC, driving OXPHOS. siSlc2a1 and BAY-876 are used for GLUT1 inhibition, while siHk2 inhibits *Hk2*. *(GLUT1, glucose transporter 1; G6P, glucose-6-phosphate; HK2, hexokinase 2; ATP, adenosine triphosphate; NADH, reduced nicotinamide adenine dinucleotide; $FADH_2$, reduced flavin adenine dinucleotide; ETC, electron transport chain; OXPHOS, oxidative phosphorylation; sSlc2a1, small interfering RNA targeting Slc2a1 (solute carrier family 2 member 1); siHk2, small interfering RNA targeting HK2)*

In recent years, researchers have increasingly recognized the crucial role of these metabolic pathways in immune cell function and how these pathways influence their activity, both in health and disease (13). For example, several studies have indicated that reprogramming the metabolism of microglia from glycolysis to OXPHOS can enhance their reparative functions in the CNS. For instance, Song et al. showed that enhanced OXPHOS activity,

achieved through a reduction in intracellular pH, ultimately improves myelin clearance and promotes post-stroke recovery. (14). Similarly, Leng et al. reported improved repair functions following enhanced amyloid-β clearance in an Alzheimer's mouse model by inducing a metabolic switch in microglia from glycolysis to OXPHOS through the inhibition of hexokinase 2 (HK2), the first key rate-limiting enzyme in glucose metabolism (15).

Furthermore, aside from augmenting phagocytosis and reducing inflammation, metabolic reprogramming of microglia from glycolysis to OXPHOS can enhance their lipid processing capabilities. Multiple studies indicated that activation of the peroxisome proliferator-activated receptor gamma (PPAR-γ), a known regulator of glucose and lipid metabolism, resulted in increased OXPHOS and a reduction in lipid droplet accumulation in microglia (7, 16). Conversely, disruption of OXPHOS has been linked to impaired lipid handling in macrophages (17). One of the pathways upstream of OXPHOS is β-oxidation, a process that degrades fatty acids to generate reducing equivalents (NADH and $FADH_2$) that participate in the electron transport chain to drive OXPHOS (Fig. 1) (13). Consequently, an increase in OXPHOS may reflect enhanced β-oxidation processes. Collectively, these findings suggest that metabolic reprogramming towards OXPHOS may represent a novel strategy to assist myelin-laden microglia in processing excess myelin, thereby facilitating remyelination.

With this study, we aim to induce metabolic reprogramming in myelin-treated macrophages from glycolysis to OXPHOS, thereby improving their myelin processing capability. This will be achieved by exploring various approaches, including the use of the inhibitor BAY-876 for the inhibition of Glucose transporter 1 (GLUT1), as well as small interfering RNAs (siRNAs) to target the transcription of GLUT1 and HK2. Both proteins serve as crucial regulators of glycolysis, with GLUT1 primarily responsible for the uptake of glucose, the primary fuel for glycolysis, into the cell cytoplasm. GLUT1 is the most prominently expressed protein in microglia (18). Meanwhile, hexokinase 2 (HK2), the first rate-limiting enzyme in the glycolysis, plays a key role in the initial breakdown of glucose into its metabolites (15). We will investigate how this metabolic reprogramming influences multiple factors, including inflammatory response, lipid load, and metabolic activity. We hypothesize that blocking glycolytic pathways in myelin-loaded macrophages will shift their metabolism towards OXPHOS, thereby improving myelin processing and promoting remyelination.

This research aims to clarify the metabolic changes in microglia observed in MS lesions and to test whether metabolic reprogramming through glycolytic inhibition can serve as a therapeutic approach to rescue foamy microglia. By doing so, it will aid in the development of innovative therapies that not only enhance repair processes through the metabolic reprogramming of microglia, but also hold the potential to find a cure for multiple sclerosis.

EXPERIMENTAL PROCEDURES

BMDM isolation – Bone marrow-derived macrophages (BMDMs) were obtained from the femur and tibia of 10–12-week-old female C57Bl/6J mice. Isolated bone marrow was cultured in RPMI 1640 medium (Gibco, 72400-021) supplemented with 10% fetal calf serum (FCS), 0.5% penicillin/streptomycin (P/S), and 15% L929-conditioned medium (LCM). Cells were differentiated for 7 days, with fresh medium added on day 4. After differentiation, BMDMs were collected and seeded at 500,000 cells/mL in RPMI 1640 medium containing 10% FCS, 0.5% P/S, and 5% LCM.

Myelin isolation and treatment – Myelin was isolated from post-mortem mouse tissue through density gradient centrifugation, as described previously (19). Myelin protein concentration was determined using the Pierce BCA Protein Assay Kit (Thermo Fisher Scientific, 23225). BMDMs were treated with myelin (100 μg/ml) for either 24h (short-term exposure), 72h (long-term exposure), or were left untreated.

BAY-876 treatments – To target glycolysis, BMDMs were treated two hours after seeding with either 500 nM of the GLUT1 inhibitor BAY-876 (Cayman, 19961-1). Cells were incubated with BAY-876 for 0.5 h prior to myelin treatment.

siRNA transfection – To knock down GLUT1 and HK2, The siRNAs siSlc2a1 (Sigma, EMU085671) and siHk2 (Sigma, EMU039591) were used, respectively, while siCtrl (Sigma, SIC001) served as a negative control. For the BMDM transfection using siRNAs, a 1:25 dilution of Lipofectamine (Invitrogen, 13778075) in Opti-MEM (Gibco, 31985-062) was prepared and incubated at room temperature for 5 minutes. An equal volume of siRNA dilution was then added. This mixture was incubated at room temperature for 20 minutes. Subsequently, the medium of the BMDMs was replaced with P/S-free RPMI medium. Finally, the prepared mix was incubated overnight in final concentration of 10 nM siRNA and 1:50 Lipofectamine.

qPCR – To determine gene expression, RNA was isolated from treated BMDMs using QIAzol reagent (Qiagen, USA, 79306) and purified using the RNeasy Mini Kit (Qiagen, 74106). RNA concentration and purity were assessed using a NanoDrop 2000 spectrophotometer (Thermo Fisher Scientific). cDNA was synthesized using qScript cDNA SuperMix (Quantabio, USA, 79306). qPCR was performed using gene-specific primers (IDT DNA; Suppl. Table 1) and SYBR™ Green Universal Master Mix (Applied Biosystems, Lithuania, 4385612) on a QuantStudio™ 3 Real-Time PCR system, with Ct values normalized to *Tbp* and *Cyca*.

Western Blot – BMDMs were lysed in RIPA buffer containing protease inhibitors (Sigma-Aldrich), and protein concentration was determined using the Pierce™ BCA Protein Assay Kit (Thermo Fisher Scientific, 23225). Equal amounts of protein (2 µg) were separated on 7.5% SDS-PAGE gels (75 V, 30 min; 200 V, 30 min) and transferred to PVDF membranes (Bio-Rad, 0.45 µm) at 300 mA for 1 h. Membranes were blocked with 5% skimmed milk in PBS-T and incubated overnight at 4°C with anti-HK2 antibody (Proteintech, 66874-1-Ig, 1:5000), followed by polyclonal rabbit anti-mouse secondary antibody (Dako, 1:5000). Signals were detected using Pierce™ ECL Plus substrate and imaged with an Amersham Imager 680 (GE Healthcare Bio-Sciences).

Immunocytochemical staining (ICC) – BMDMs were fixed on glass coverslips with 4% paraformaldehyde for 15 min, permeabilized with 0.1% Triton in PBS, and blocked for 1 h with protein block (Dako, X0909). Cells were incubated overnight at 4 °C with primary antibodies against HK2 (Proteintech, 66974-1-Ig, 1:750) and F4/80 (Biorad, MCA4972, 1:1000), followed by Donkey anti-mouse 555 and Donkey anti-rat 647 secondary antibodies (1:400). Lipid droplets were stained with Bodipy (2 µM, 30 min) and nuclei with DAPI. Slides were mounted with fluorescence mounting medium, imaged at 40× magnification using a Leica DM4000 B microscope, and analyzed using Fiji (ImageJ, version 2.14.0).

Oil Red O (ORO) staining – BMDMs were cultured on glass cover slides and fixed in 4% paraformaldehyde (PFA) for 10 min. To stain intracellular neutral lipids, BMDMs were incubated with 0.3% ORO working solution for 10 min at RT. After the slides were washed with tap water, cells were counterstained with heamatoxylin for 1 min and rinsed in running tap water for 5 min. Analysis was performed with Leica DM2000 LED microscope (Leica Microsystems) and Fiji software (ImageJ, version 2.14.0).

Nitric oxide (NO) assay – NO production was assessed by measuring nitrite levels in culture supernatants of LPS-stimulated (100 ng/mL, overnight) BMDMs using the Griess reagent system. Equal volumes of supernatant and a 1:1 mixture of solution A (0.1% N-(1-naphthyl)ethylenediamine; Sigma N5889) and solution B (2.5% H_3PO_4, 1% sulfanilamide; Sigma S9251) were combined, and absorbance was measured at 540 nm using a CLARIOstar PLUS microplate reader (BMG Labtech). Nitrite concentrations were derived from a 100 µM sodium nitrite standard curve.

MTT assay – Mitochondrial activity in treated BMDMs was assessed using the MTT assay. MTT working solution (5 mg/ml) was added to all wells and incubated for 4 h at 37°C, 5% CO_2. After incubation, the medium was replaced with an 85% DMSO–15 mM glycine solution (150 µL DMSO and 25 µL glycine solution [0.1 M glycine, 0.1 M NaCl]) to dissolve formazan crystals. Absorbance was measured at 550 nm using a CLARIOstar PLUS microplate reader (BMG Labtech).

ROS assay – To measure ROS production in BMDMs, 100 µL of diluted DCFH (10 µM) was added and incubated for 30 minutes at 37°C. Following incubation, the DCFH solution was replaced with PBS, and fluorescence was measured using the CLARIOstar PLUS microplate reader (BMG Labtech) at an excitation wavelength of 485 nm.

BSC culture and staining – Cerebellar brain slices were isolated from P10–P11 pups and cultured on inserts in 6-well plates containing BSC medium. Macrophages were depleted the following day using clodronate liposomes (Liposoma, 1:10) for 24 h, followed by repletion with siRNA-treated macrophages. Demyelination was induced with lysophosphatidylcholine (LPC, Sigma, L4129, 0.5 mg/ml). Slices were fixed with 4% PFA on day 3 (demyelination) or day 12 (remyelination). Following fixation, slices were stained overnight at 4°C with antibodies against MBP (Rat anti-MBP, MCA409S, 1:250) and NF (Rabbit anti-NF, Ab8135, 1:1000) and imaged using an LSM900 Airyscan 2 Confocal microscope (Zeiss, Belgium).

Extracellular flux assay – BMDMs were seeded onto Seahorse XF Pro M cell culture microplates (Agilent, 103774-100) and treated with myelin together with either BAY-876 or siRNAs as described. One hour prior to the assay, medium was replaced with RPMI-based Seahorse XF medium (Agilent, 103575-100) supplemented with 2 mM glutamine (Agilent 103579-100) and 1 mM pyruvate (Thermo Fisher, 11360070), followed by incubation for 1 h at 37°C in a non-CO_2 incubator. Oxygen consumption rate (OCR) and extracellular acidification rate (ECAR) were measured using a Seahorse extracellular flux analyzer (Agilent). OCR responses were assessed using oligomycin (1.5 µM), FCCP (1.5 µM), and antimycin A/rotenone (2.5 µM/1.25 µM) to evaluate mitochondrial respiration, while ECAR changes in response to 10 mM glucose (Sigma, G8769) were used to assess glycolysis. Fuel dependency was evaluated using etomoxir (1 µM), BPTES (2 µM), UK5099 (3 µM), and 2-DG (50 mM), examining dependence on fatty acids, glutamine, pyruvate, and glucose, respectively; the medium was additionally supplemented with 10 mM glucose. Hoechst (50 µg/ml, Thermo Fisher, 33342) was added for cell number normalization using a Nikon confocal microscope with a 96-well plate cell quant loop. Data were analyzed using Wave software (v2.6.0.3).

Flow cytometry (Mitotracker, BODIPY) – BODIPY and Mitotracker stainings were used to assess lipid accumulation and mitochondrial quantity in treated BMDMs, respectively. Cells were incubated with Mitotracker (100 nM in RPMI, 30 min) or BODIPY (2 µM, 15 min), washed with PBS, and analyzed using an LSR Fortessa Flow Cytometer (488 nm). Data were processed using FlowJo software (v10.10.1).

Statistical analysis – Data were analyzed using GraphPad Prism v10 (GraphPad Software, USA) and are presented as mean ± SEM unless stated otherwise. Normality was assessed using the Shapiro–Wilk test. Multiple-group comparisons were performed using one-way ANOVA or Kruskal–Wallis tests, followed by Tukey's or Dunn's multiple comparisons tests, respectively. $P < 0.05$ was considered statistically significant (*$P < 0.05$, **$P < 0.01$, ***$P < 0.001$, ****$P < 0.0001$).

RESULTS

Myelin treatment of BMDMs elevates both glycolysis and mitochondrial respiration – Understanding the metabolic changes that macrophages undergo upon myelin uptake can provide valuable insights into the pathology of MS and could reveal potential therapeutic targets in this understudied area. To elucidate these metabolic changes, an extracellular flux (XF) assay was employed for real-time monitoring of metabolic activity in response to both short- and long-term myelin exposure. This assay quantifies the extracellular acidification rate (ECAR), which signifies glycolytic activity, primarily due to lactate efflux. Concurrently, the oxygen consumption rate (OCR) is assessed, which serves as an indicator of mitochondrial respiration. XF analysis revealed a significant increase in glycolysis in BMDMs treated with myelin for both 24 and 72 hours, with the most pronounced increase observed at the 72-hour mark. Additionally, OCR also increased significantly, indicating that myelin treatment enhanced the basal respiration of the cells (Figure 2D). Furthermore, different inhibitors that target the ETC in various ways were employed to obtain additional readouts from this assay. Oligomycin, which targets ATP synthase

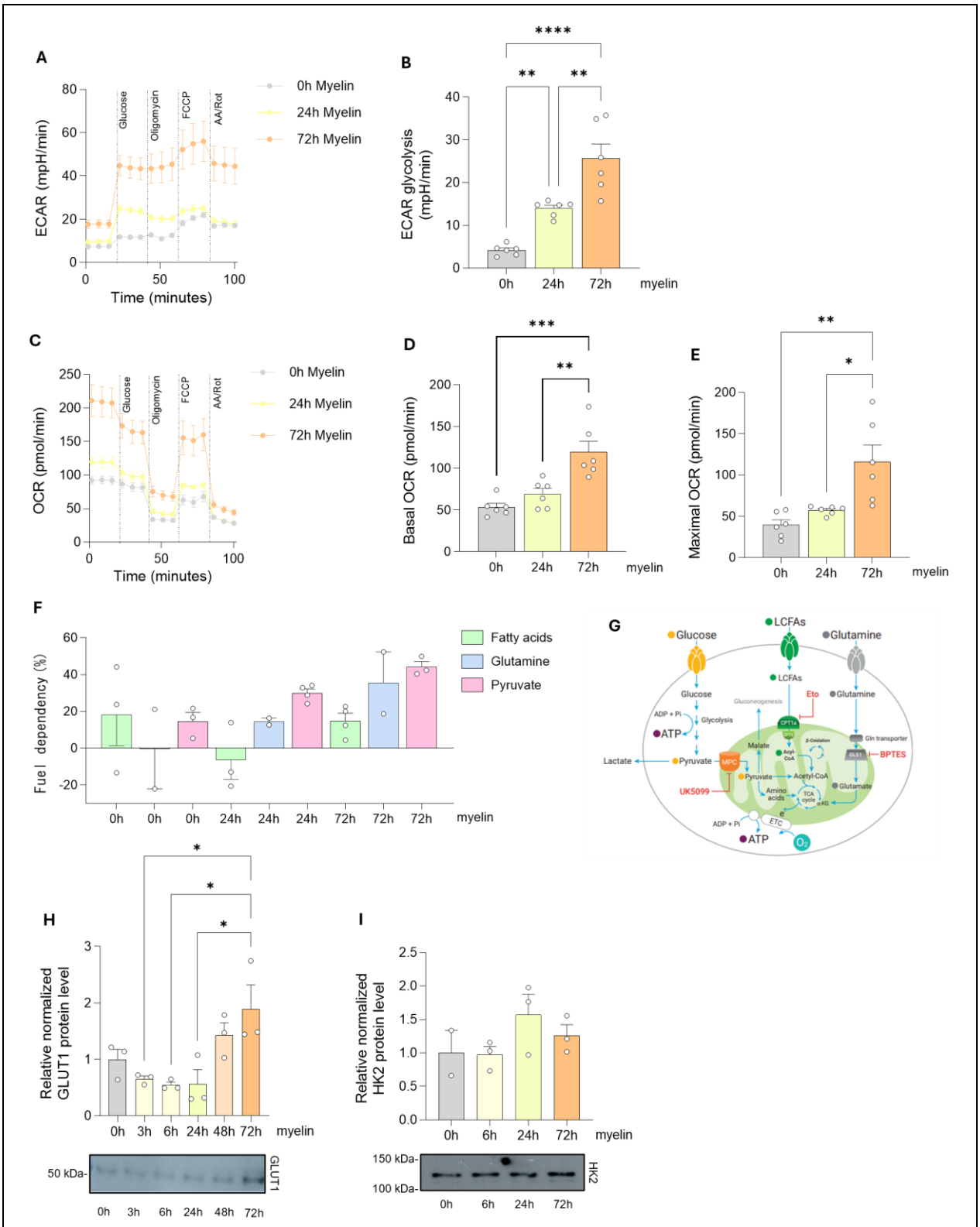

Fig. 2 : Myelin treatment of BMDMs elevates both the glycolysis and mitochondrial respiration. (A-F) BMDMs were treated with myelin (100 µg/ml) for 24 h (short-term exposure) or 72 h (long-term exposure), the control group did not receive myelin. (A, B) The extracellular flux assay shows the significant increase of ECAR values, indicating glycolytic activity, upon myelin treatment for both the 24 h and 72 h timepoints. (C-E) The OCR measurement also revealed a significant elevation in mitochondrial respiration after treatment. (F) Fuel dependency test with the inhibitors Etomoxir (1 µM), BPTES (2 µM), and UK5099 (3 µM) to inhibit fatty acid, glutamine, and glucose uptake into the mitochondria, respectively. (G) Schematic overview of cell metabolism and fuel dependency test. (H,I) Western Blot analysis show a significant increase of GLUT1 protein levels in myelin treated cells, while the HK2 protein levels were not noticeably elevated. Results are presented as Mean ±SEM, n=3. One-way ANOVA and Kruskal-Wallis test with Tukey's and Dunn's correction, respectively. *(BMDMs, bone marrow-derived macrophages; ECAR, extracellular acidification rate; OCR, oxygen consumption rate; GLUT1, Glucose Transporter Type 1; HK2, hexokinase 1; AA/Rot, Antimycin A/Rotenone)*

(Complex V of the electron transport chain), and FCCP were used, along with a combination of Antimycin A and Rotenone to inhibit Complexes I and III, respectively (Fig. 2E). Furthermore, the addition of FCCP causes the collapse of the proton gradient that drives the ETC, thereby allowing the extraction of the maximal respiration data (Fig. 2E). To further characterize the fuel sources, main fuel pathways were inhibited to study the dependency on fatty acids (CPT1A inhibitor; Etomoxir), pyruvate (MPC inhibitor; UK5099) and glutamine (glutaminase; BPTES). Fatty acids do not appear to be critical as fuel sources, as evidenced by their dependency alongside glutamine mostly remaining below 20%. In contrast, the dependency on pyruvate is noticeably higher, suggesting that pyruvate, and therefore gl[SV12.1]ycolysis, serves as a primary fuel supply in the myelin-treated BMDMs (Fig. 2F). Additionally, protein levels of GLUT1, responsible for glucose uptake, and HK2, the first rate-limiting enzyme in the glycolytic pathway, were assessed through Western blot analysis to evaluate their involvement in the changes observed in glycolytic activity. The data indicates a significant upregulation of GLUT1, whereas HK2 levels exhibited minimal variation, with only a slight elevation observed (Fig. 2G, H).

GLUT1 inhibition with BAY-876 suppresses glycolysis in myelin-treated BMDMs. – Since the most noticeable changes were observed in glycolytic activity after 72 hours of myelin treatment, we hypothesize that increased glycolysis may be linked to phagocyte dysfunction. To evaluate the role of this pathway, BAY-876 was used to target GLUT1, thereby inhibiting glucose uptake and subsequently glycolysis. An extracellular flux assay was conducted to determine whether this approach could suppress the increased glycolytic activity in the myelin-treated cells (Fig. 3A, B). The inhibition by BAY-876 generally reduced glycolytic activity across all conditions, with a significant decrease noted in the 72 h treated groups (Fig. 3B). To further investigate the metabolic flexibility of the BMDMs in response to the inhibition of glucose uptake via GLUT1, a fuel dependency test was performed (Fig. 3A-E). Inhibition of glucose uptake did not result in the cells adopting fatty acids as an alternative fuel source (Fig. 3C). Inhibiting GLUT1 slightly reduced the utilization glutamine and pyruvate as fuel sources, with pyruvate, and thus glycolysis, showing a noticeable decline as a fuel option in the 72 h myelin-treated cells incubated with BAY-876 (Fig. 3E). To assess how the inhibition of glycolysis by targeting GLUT1 with BAY-876 affected the glycolytic profile of the cells, qPCR and ICC analyses were performed to evaluate both GLUT1 and HK2 expressions (Fig. 3F-I). In BMDMs that did not receive myelin, the introduction of BAY-876 resulted in an upregulation of the GLUT1 coding gene *Slc2a1*, paired with a significant increase at the protein level. However, the differences in expression upon BAY-876 treatment diminished when myelin was introduced (Fig. 3F, G). Additionally, protein levels of HK2 also significantly increased in the BAY-876 treated group that did not receive myelin (Fig. 3I). This suggests that a compensatory mechanism is activated when glucose uptake is inhibited.

siRNA-mediated knockdown of Slc2a1 and Hk2 succesfully reduce glycolysis – For a more targeted approach, BMDMs were transfected overnight with small interfering RNAs (siRNAs) silencing *Slc2a1* (siSlc2a1) and *Hk2* (siHk2) to interfere with GLUT1 and HK2, respectively, thereby disrupting glycolysis at different levels. ECAR values following glucose injection indicated a significant decrease in glycolytic activity in the cells treated with both siRNAs compared to the siCtlr-transfected groups (Fig. 4A, B). Additionally, the changes in fuel dependency due to reduced glycolysis were evaluated to determine whether there was a metabolic shift to a different pathway. The 24-hour treated BMDMs with *Hk2* knockdown demonstrated a reduced dependence on fatty acids, glutamine, and pyruvate as energy sources compared to the *Slc2a1* knockdown. However, pyruvate remained the preferred fuel under these conditions, indicating that the knockdown of both *Slc2a1* and *Hk2* did not alter the fuel dependency in these cells.(Fig. 4-E). Additionally, changes in the expression of *Slc2a1* and *Hk2* were measured under the different conditions. The downregulation of their transcription in the no myelin-treated groups confirms gene silencing by the siRNAs (Fig. 4F, G). In the myelin-treated groups, *Slc2a1* expression was elevated in response to *Slc2a1* knockdown. while myelin exposure did

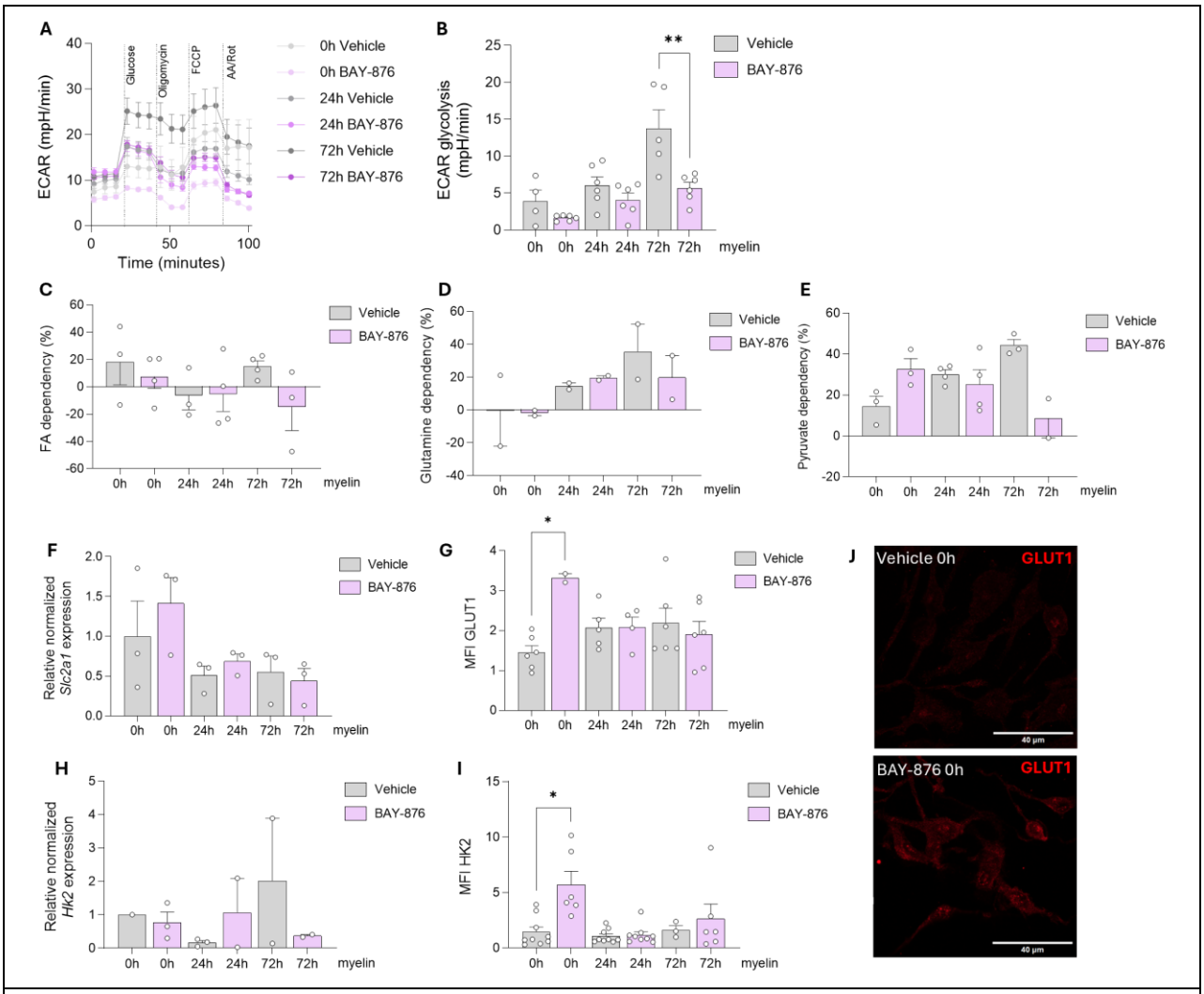

Fig. 3 – GLUT1 inhibition with BAY-876 suppresses glycolysis in myelin-treated BMDMs. (A-I) Changes in glycolytic metabolism were observed in BMDMs treated with BAY-876 compared to control groups. Myelin treatments were administered for 24 h or 72 h, the control groups did not receive myelin (A,B). The extracellular flux assay indicated a significant decrease in extracellular acidification rate (ECAR) in BMDMs treated for 72 h (C-E). The dependence on fatty acids, glutamine, and pyruvate in the treated cells was analyzed in comparison to the vehicle groups. (F,G) Transcriptional changes and protein levels of GLUT1, encoded by *Slc2a1*, were evaluated. (H,I) The expression of HK2 was assessed at both transcriptional and protein levels. (J) Representative images of GLUT1 staining, scale bar = 40µm. Data are presented as Mean ±SEM, n=3. One-way ANOVA and Kruskal-Wallis test with Tukey's and Dunn's correction, respectively. *(BMDMs, bone marrow-derived macrophages; ECAR, extracellular acidification rate; GLUT1, Glucose Transporter Type 1; HK2, hexokinase 1; AA/Rot, Antimycin A/Rotenone); FA, fatty acid; MFI, mean fluorescence intensity)*

not affect *Slc2a1* expression in the siHk2 treated groups (Fig. 4F). As for *Hk2* expression, a minimal downward trend was observed across all conditions following the knockdowns (Fig. 4G).

Targeting glycolysis negatively affects mitochondrial health, hindering improvements in mitochondrial respiration. – The extracellular efflux results from BMDMs treated with BAY-876 and siRNAs demonstrated that glycolytic activity was successfully targeted, it did not enhance mitochondrial respiration. Instead, maximal respiration even decreased significantly in the myelin-treated cells with siSlc2a1 and siHK2 (Fig. 5A-F). Therefore, whether the BAY-876 and siRNA treatments influenced mitochondrial mass and function in the cells was evaluated. To assess changes in mitochondrial mass, the incorporation of the fluorescent probe MitoTracker was measured by flow cytometry.

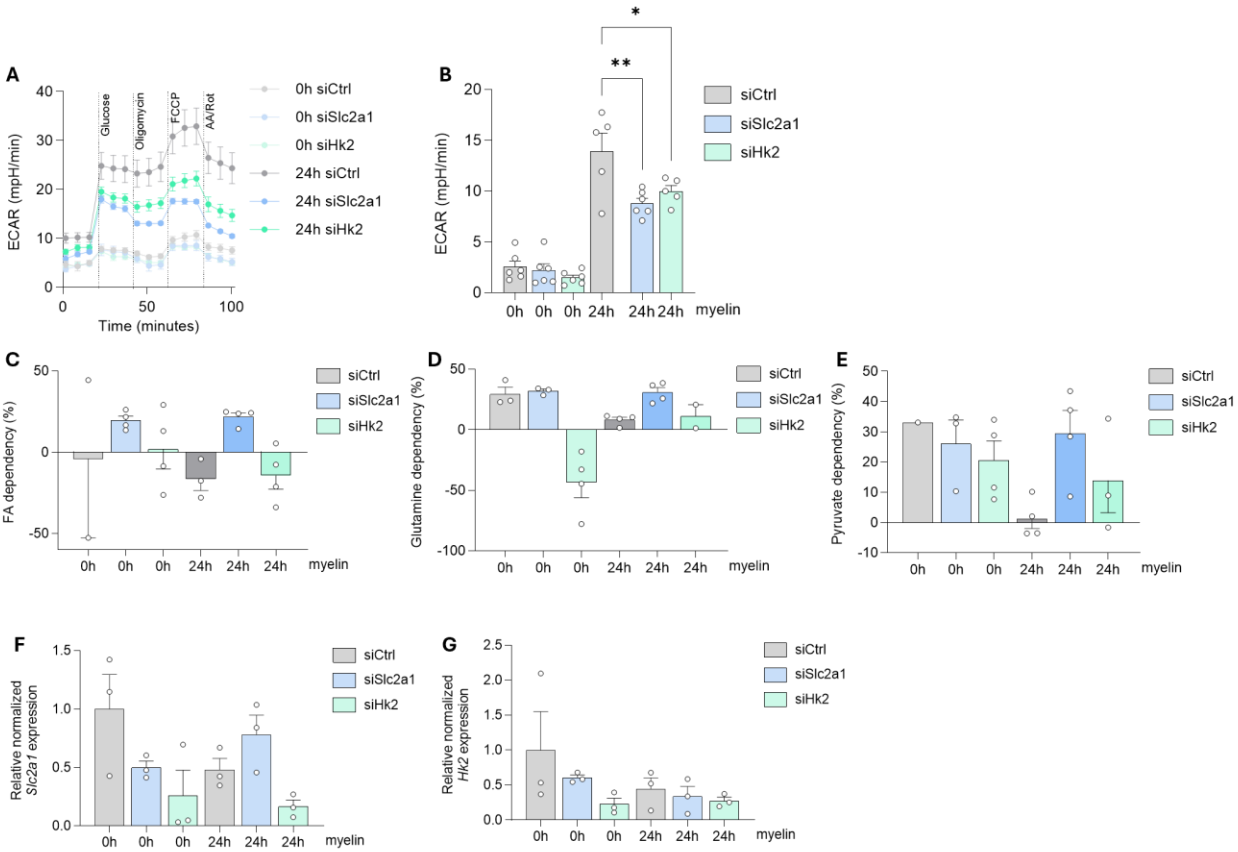

Fig. 4 – Inhibition of glycolysis is also achieved following specific inhibition of *Slc2a1* and *Hk2* using siRNAs. (A,B) ECAR values and fuel dependency assessment derived from the extracellular flux assay of BMDMs transfected overnight with siSlc2a1 to affect GLUT1 expression and siHk2 to affect HK2, including an additional myelin treatment for a duration of 24h. siCtrl transfected BMDMs were used as the control group. (C-E) Dependancy of FA, glutamine, and pyruvate fuels, illustrated by the changes in maximal respiration after the addition of inhibitors Etomoxir, BPTES, and UK5099, respectively. (F,G) Changes in gene expression of *Slc2a1* and Hk2 across the different conditions, with results normalized to the housekeeping genes *Tbp* and *Cyca*. Data are presented as Mean ±SEM, n=3. One-way ANOVA and Kruskal-Wallis test with Tukey's and Dunn's correction, respectively. *p<0.05; **p<0.01 *(BMDMs, bone marrow-derived macrophages; ECAR, extracellular acidification rate; GLUT1, Glucose Transporter Type 1; HK2, hexokinase 1; AA/Rot, Antimycin A/Rotenone); FA, fatty acid; Slc2a1, Solute Carrier Family 2 Member 1)*

BAY-876 treated cells indicated an upward trend in mitochondrial signal for the 24-hour treatment group and a downward trend for the 72-hour group (Fig. 5G). In contrast, BMDMs transfected with siHk2 and treated for 24 hours exhibited a significant increase in MitoTracker fluorescence, suggesting an increase in mitochondrial mass, while no notable changes were observed in other conditions (Fig. 5J). Furthermore, an MTT was employed to evaluate mitochondrial activity. Comparing the control groups revealed that myelin treatment alone seems to enhance mitochondrial activity. In line with XF analyses, both BAY-876 and siRNAs decreased mitochondrial activity in the myelin-treated groups (Fig. 5H, K). Additionally, ROS production was assessed by DCFH, which showed a decrease in controls receiving short-term myelin exposure, whereas prolonged exposure stimulated ROS production. Inhibition of GLUT1 by BAY-876 showed an overall trend to increased ROS production across all myelin conditions, while siHk2 and siSlc2a1 did not affect ROS. (Fig. 5I, L)

Inhibition of glycolysis shifts the phenotype of myelin-treated BMDMs towards an anti-inflammatory state. – An inflammatory response is typically associated with increased glycolytic activity. Therefore, we aimed to evaluate whether alterations in glycolytic activity in the treated cells reflect their inflammatory response. Therefore, the levels of

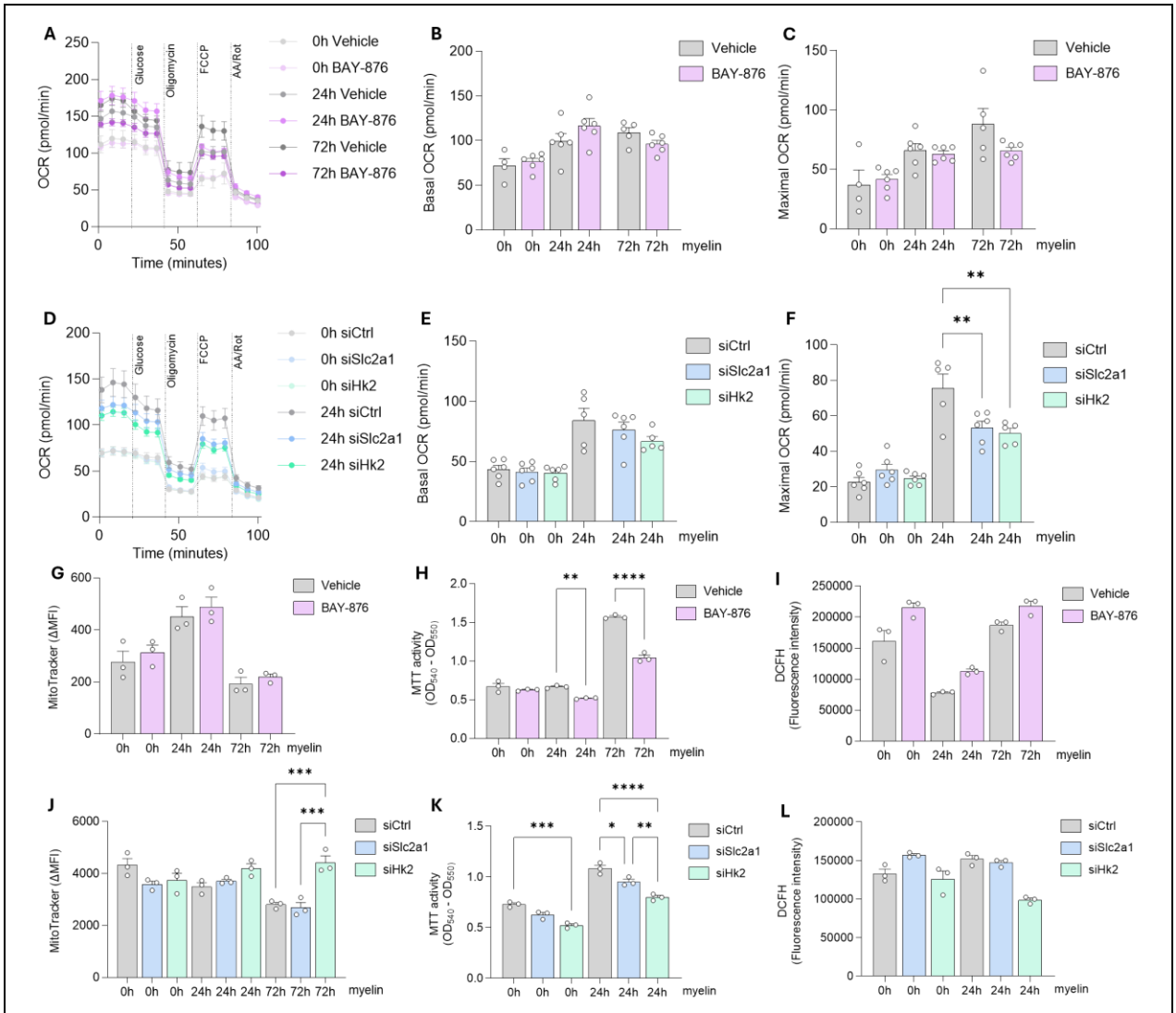

Fig. 5 – Targeting glycolysis negatively affects mitochondrial health, hindering improvements in mitochondrial respiration. (A) OCR values measured by extracellular flux assay of BMDMs with BAY-876 (500nM) and myelin treatments, including the (B) basal and (C) maximal respiration data acquired following FCCP injection, normalized for cell count. (D-F) Normalized OCR obtained from cells transfected overnight with siSlc2a1 or siHk2 (10nM), along with myelin-treated groups. siCtrl-transfected cells were used as a control. (G) FACS analysis results using the MitoTracker fluorescent probe (100 µM), which targets mitochondria. ΔMFI was calculated by (H) MTT assay and (I) ROS assay for the evaluation of mitochondrial health in cells treated with BAY-876. (J-L) Assessment of mitochondrial mass and health of siRNA-transfected cells using FACS, MTT, and ROS measurements, respectively. Results are presented as Mean ±SEM, n=3. One-way ANOVA and Kruskal-Wallis test with Tukey's and Dunn's correction, respectively. *p<0.05; **p<0.01; ***p<0.001; ****p<0.0001 *(BMDMs, bone marrow-derived macrophages; OCR, oxygen consumption rate; GLUT1, Glucose Transporter Type 1; HK2, hexokinase 1; AA/Rot, Antimycin A/Rotenone; FACS, Fluorescence-Activated Cell Sorting; MTT, 3-(4,5-dimethylthiazol-2-yl)-2,5-diphenyltetrazolium bromide; ROS, reactive oxygen species; A.U., arbitrary unit; MFI, mean fluorescence intensity; FCCP, Carbonyl cyanide 4-(trifluoromethoxy)phenylhydrazone)*

NO production and inflammatory gene expressions were measured for each condition after activating the inflammatory response using LPS and IFNγ. Both GLUT1 inhibition and siRNA-mediated knockdown of *Slc2a1* and Hk2 were able to reduce inflammatory activation in 24 and 72h treated cells (Fig. 6A, F). The reduction of NO was also reflected at the transcriptional level, with *Nos2* levels going down, which codes for the iNOS enzyme responsible for NO production (Fig. 6B, G). As for interleukin-6 (*Il6*), *Il1b*, and tumor necrosis

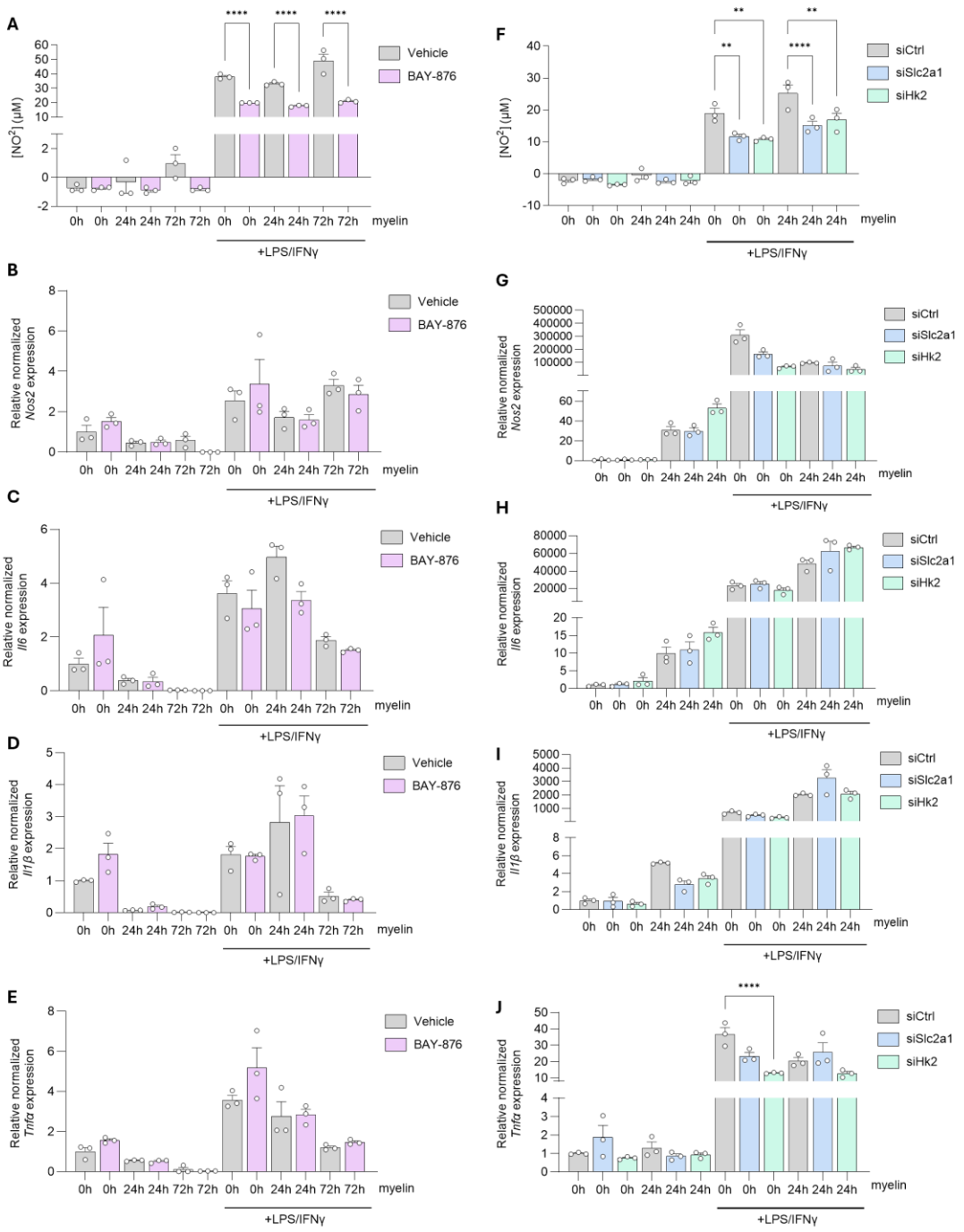

Fig. 6 – Inhibition of glycolysis shifts the phenotype of myelin-treated BMDMs towards an anti-inflammatory state. (A-E) Experimental conditions consisted of BMDMs exposed to myelin for 0, 24, or 72h, in the presence of either vehicle or BAY-876. For each condition, parallel samples were either left untreated or stimulated with LPS and IFNγ for 6h. (A) NO production in response to Bay-876 treatment. qPCR analysis of Bay-876 treated samples, normalized to *Tbp* and *Cyca*, of genes involved in inflammation, including (B) *Il6*, (C) *Nos2*, (D) Il1β, and (E) *Tnf*α. (F-J) BMDMs transfected with either siCtrl, siSlc2a1, or siHk2 were exposed to either no myelin or myelin for 24 hours, with some conditions also receiving additional LPS and IFNg. (F) No production was assessed in the experimental groups treated with siRNAs. (G-J) Measured transcriptional changes of inflammatory genes in response to siRNA transfection, with *Tbp* and *Cyca* used for normalization. Results are presented as Mean ±SEM, n=3. One-way ANOVA and Kruskal-Wallis test with Tukey's and Dunn's correction, respectively. *p<0.05; **p<0.01; ***p<0.001; ****p<0.0001 *(BMDMs, bone marrow-derived macrophages; NO, nitric oxide; LPS, Lipopolysaccharide; IFNγ, Interferon-γ; Il6, Interleukin-6; Nos2, Nitric oxide synthase; Il1β, Interleukin-1β; Tnfα, Tumor necrosis factor-α)*

factor alpha (*Tnfα*), all of which code for pro-inflammatory cytokines. BAY-876 and siRNAs had no, or a minimal effect on their expression. As for interleukin-6 (*Il6*), *Il1b*, and tumor necrosis factor alpha (*Tnfα*), all of which code for pro-inflammatory cytokines,, BAY-876 and siRNAs showed little to no impact on their expression (Fig. 6C-E, 6G-I).

Suppressing glycolysis exacerbates lipid load in long-term myelin-treated BMDMs. – To investigate whether inhibiting glycolytic activity enhances the ability to manage lipid overload, the effects of BAY-876 and siRNA treatments on lipid droplets and their processing were evaluated at both functional and transcriptional levels.Lipid levels were estimated by Oil Red O (ORO) staining within the cells under varying conditions. This analysis confirmed lipid accumulation in cells treated with myelin. However, it did not demonstrate any significant effects of the inhibition and siRNA-mediated knockdown on lipid load (Fig. 7A). Additionally, ICC and FACS using the fluorescent probe BODIPY, which also stains neutral lipids, were employed to further evaluate lipid load. Both methods showed an overall increasing trend in lipid load with longer treatment durations. Notably, when comparing the vehicle group to the BAY-876-treated group exposed to myelin for 72 hours, the BAY-876 group exhibited a higher accumulation of lipids (Fig. 7B, C). Further evaluation using ORO and FACS with BODIPY was conducted in the siRNA-treated groups, revealing results comparable to those of the BAY-876 treatment. However, under long-term exposure conditions, siHK2 appeared to contribute to greater lipid accumulation compared to siSlc2a1, which targets GLUT1 (Fig. 7D, E). To investigate the impact of the treatments on gene transcription related to lipid handling or lipid droplets, qPCR analysis was performed (Fig. 7F-K). *Cd36* encodes a lipid transporter responsible for lipid uptake into cells and exhibited a slight and steady upregulation with increasing myelin exposure. Conversely, the transfected cells displayed a downward trend in *Cd36* expression when treated with myelin for 24 hours (Fig. 7I). Given that a significant portion of myelin is composed of cholesterol, *Abca1* expression was analyzed due to its role in cholesterol efflux. Interestingly, while BAY-876 did not affect *Abca1* expression at 0 and 24 hours, a significant increase in Abca1 expression was observed after 72-hour BAY-876 treatment. (Fig. 7G). In contrast to BAY-treatment, siRNA mediated knockdown of *Hk2* and *Slc2a1* slightly reduced Abca1 expression after 24h myelin treatment(Fig. 7J). Lastly, the integrity of the lipid droplets was assessed with *Plin2*, as it codes for a surface protein of lipid droplets involved in their stabilization. Results from BAY-876 treatments indicated an overall upward trend in *Plin2* expression, (Fig. 7H). In contrast, *Plin2* expression in siRNA-transfected cells showed minimal changes (Fig. 7K).

Replacement of macrophages with siRNA transfected BMDMs did not improve remyelination in BSCs. – To assess the effect of glycolysis inhibition on remyelination, brain slice cultures repleted with siRNA-treated BMDMs were subjected to LPC-induced demyelination. Following demyelination, myelination indices were slightly lower in repleted cultures than in the non-depleted control condition. However, after the remyelination period, myelination indices reached comparable levels across all conditions, and no clear treatment-related differences were observed (Fig. 8B). Additionally, plotting the differences between myelination indices of remyelination and demyelination also showed a much lower remyelination capacity of the siScl2a1 and siHk2 treated groups, compared to the siCtrl group (Fig. 8C).

DISCUSSION

Current literature highlights the importance of immunometabolism in understanding the pathophysiology of diseases. Investigating the immunometabolism of cells in various pathologies has increasingly been recognized as a valuable approach, potentially revealing new therapeutic targets (13, 14, 20). Therefore, it is crucial to understand how the metabolism of macrophages changes in response to myelin treatment, both in the short term and long term. Our study demonstrated significant increases in glycolysis and mitochondrial respiration in cells treated with myelin for both 24 hours and 72 hours, with the greatest increase in glycolysis observed at the 72-hour mark. This suggests that these cells are overall activated metabolically by myelin. Earlier evidence indicates that disease-associated macrophages and microglia often exhibit heightened glycolytic activity, typically accompanied by an

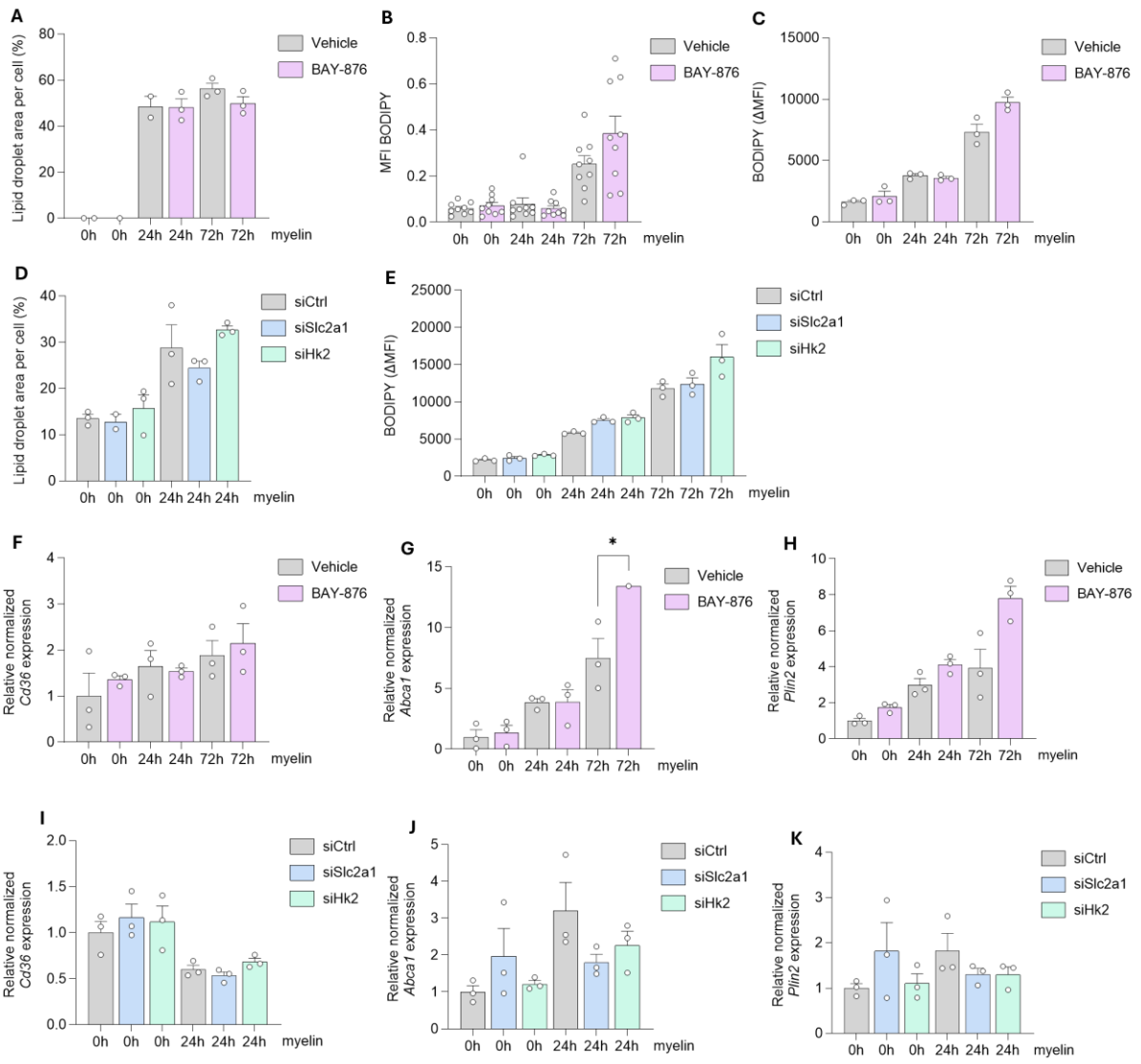

Fig. 7 – Suppressing glycolysis appears to exacerbate lipid load in long-term myelin-treated BMDMs. (A, D) ORO staining was performed to visualize neutral lipids in cells incubated with either vehicle or BAY-876, or transfected overnight with siRNAs, and exposed to myelin for durations of 0h, 24h, or 72h. Data were normalized to cell count. (B) Lipid droplets were stained through immunocytochemistry (ICC) using BODIPY, DAPI staining of the nuclei was used to normalize for nuclei count (C) Median fluorescence measurements of BODIPY were obtained using FACS. Both ICC and FACS indicated an upward trend in BODIPY fluorescence corresponding with the duration of myelin exposure. (E) FACS analysis displayed median fluorescence of BODIPY in siRNA-transfected cells exposed to either 0h or 24h of myelin. (F-H) qPCR analysis of target genes *Cd36, Abca1,* and *Plin2* was conducted to evaluate transcription related to lipid uptake, cholesterol efflux, and lipid droplet stability in response to BAY-876 and myelin treatments. (I-K) qPCR analysis of *Cd36, Abca1,* and *Plin2* in bone marrow-derived macrophages (BMDMs) transfected overnight with siSlc2a1 or siHk2 was performed, and data were normalized to the housekeeping genes *Tbp* and *Cyca*. Results are presented as Mean ±SEM, n=3. One-way ANOVA and Kruskal-Wallis test with Tukey's and Dunn's correction, respectively. *p<0.05 *(BMDMs, bone marrow-derived macrophages; MFI, mean fluorescence intensity;ICC, immunocytochemistry; FACS, fluorescence-activated cell sorting; CD36, cluster of differentiation 36 (also known as fatty acid translocase); ABCA1, ATP-binding cassette subfamily A member 1; PLIN2, perilipin 2; BODIPY, boron-dipyrromethene (boron-dipyrromethene fluorescent dye); DAPI, 4',6-diamidino-2-phenylindole.)*

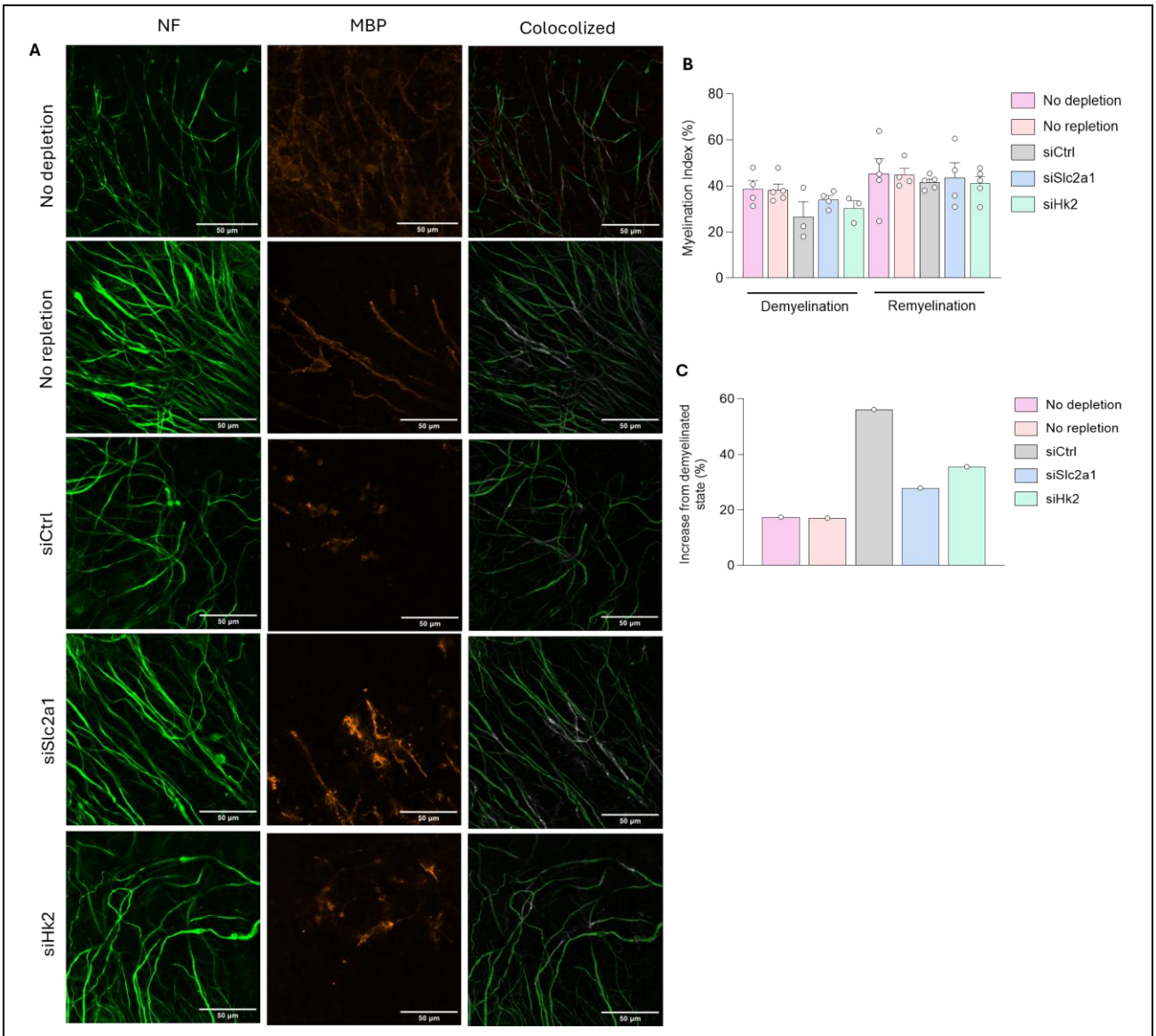

Fig. 8 – Replacement of macrophages with siRNA transfected BMDMs did not improve remyelination in brain slice cultures. (A) Representative BSC images, scal bar = 50µm. (B) BSCs were isolated from P10 to P11 pups and depleted of macrophages. Each BSC received a replacement of 4000 macrophages that were transfected overnight with either siCtrl, siSlc2a1, or siHk2. A group without depletion and repletion served as the baseline and negative control, respectively (n=3-5 BSCs per condition). On day 5, demyelination was induced by adding 0.5 mg/ml LPC to each slice. One set of conditions was fixed a day after demyelination, while another set was fixed on day 12. Three images were captured per BSC using LSM900, and the Myelination index was analyzed and plotted as Mean ±SEM. (C) Difference between myelination indices between remyelination and demyelination. One-way ANOVA test with Tukey's. *(BMDMs, bone marrow-derived macrophages; BSC, brain slice culture; LPC, lysophosphatidylcholine)*

, typically accompanied by an inflammatory response, while oxidative phosphorylation is downregulated (13, 21, 22). However, there is limited knowledge about the metabolic reprogramming in myelin-laden macrophages. Qin et al. (2023) found that there was an increase in the expression of glycolytic genes upon myelin exposure in microglia, correlating with a rise in genes associated with inflammation. In contrast, genes related to oxidative phosphorylation and fatty acid oxidation were slightly downregulated. Notably, 48 hours after stimulation with myelin debris, oxidative phosphorylation levels increased, suggesting a pro-repair phenotype (7).

Due to the heightened glycolytic activity, lactylation is a process that warrants further investigation. Previous research indicates that

lactylation can establish a positive feedback loop, further stimulating glycolysis. Moreover, both NO and hypoxia-inducible factor 1-alpha (HIF-1α) inhibit pyruvate dehydrogenase, compelling cells to rely solely on glycolysis as their energy source. This mechanism may help explain the observed dependence on pyruvate across various conditions (23, 24).

To initiate the reprogramming process, GLUT1 and HK2 were selected as targets for inhibition due to their protein levels being upregulated following myelin treatment. Inhibiting GLUT1 and HK2 using BAY-876, siSlc2a1, and siHk2, respectively, effectively resulted in the suppression of glycolysis. However, contrary to expectations, this inhibition did not lead to a reprogramming of metabolism towards an increase in OXPHOS, which is typically associated with pro-repair characteristics (14, 15).

While metabolic reprogramming of macrophages can be achieved through various strategies, shifting from increased glycolysis to enhanced OXPHOS that yields beneficial therapeutic effects, optimizing our targeting approach is essential to fully harness the therapeutic potential of metabolic reprogramming.

Furthermore, it is possible that the treatments may adversely impact mitochondrial health, potentially hindering mitochondrial respiration capacity. Interestingly, both BAY-876 and siRNA treatments appeared to significantly reduce mitochondrial activity. Additionally, levels of reactive oxygen species (ROS) were also assessed. In the case of BAY-876, ROS levels exhibited an upward trend compared to the controls, suggesting that elevated ROS levels could contribute to oxidative stress, which may subsequently affect mitochondrial health and impair its function. This could explain the cells' inability to upregulate their mitochondrial respiration (25). In contrast, the ROS production in siRNA-transfected cells did not show an increase; instead, it even slightly decreased in the siHK2 group.

Ultimately, the goal of metabolic reprogramming is to assist cells in managing their lipid overload, thereby reducing the lipid burden and facilitating recovery. An intriguing observation from multiple assays was that, at the 72-hour mark in the myelin treatment group, the lipid load appeared to worsen when using the inhibitors, both BAY-876 and siRNAs, instead of decreasing. This could indicate that glycolysis plays a crucial role in the processing of lipid droplets. However, the extent and nature of this involvement remain unclear. Notably, treatment with BAY-876 at 72 hours resulted in a significant upregulation of PLIN2, a gene that encodes surface proteins on lipid droplets that are crucial for their formation and stabilization. Elevated PLIN2 levels are associated with increased lipid loads and poorer remyelination (26). Additionally, the lack of improvement in myelination in the BSCs treated with siRNA-transfected BMDMs further supports the conclusion that these treatments are ineffective in reducing lipid load and enhancing remyelination.

The traditional M1 and M2 classification is increasingly being set aside in favor of recognizing a broader array of microglial subsets identified in disease models (27). Overall, macrophages appear to adopt a highly complex and dynamic phenotype in response to various treatments, including myelin, BAY-876, and siRNA transfections. Rather than producing a purely damaging or reparative phenotype, these approaches tend to exhibit both characteristics simultaneously. For instance, two distinct microglial subsets have been observed in active lesions: one exhibits enhanced phagocytosis and an inflammatory response, while the other displays a more pro-remyelination phenotype, characterized by elevated levels of genes associated with myelin formation and maintenance (7).

CONCLUSION

The results obtained from this research indicate that while metabolic reprogramming of macrophages has significant therapeutic potential to shift the metabolism of myelin-loaded macrophages from a damaging phenotype to a reparative one, further optimization is necessary to improve lipid processing and enhance remyelination.

REFERENCES

1. Walton, C., King, R., Rechtman, L., Kaye, W., Leray, E., Marrie, R. A. *et al.* (2020) Rising prevalence of multiple sclerosis worldwide: Insights from the Atlas of MS, third edition Mult Scler **26**, 1816-1821 10.1177/1352458520970841
2. Murta, V., andFerrari, C. C. (2013) Influence of Peripheral inflammation on the progression of multiple sclerosis: evidence from the clinic and experimental animal models Mol Cell Neurosci **53**, 6-13 10.1016/j.mcn.2012.06.004
3. Rida Zainab, S., Zeb Khan, J., Khalid Tipu, M., Jahan, F., andIrshad, N. (2025) A review on multiple sclerosis: Unravelling the complexities of pathogenesis, progression, mechanisms and therapeutic innovations Neuroscience **567**, 133-149 10.1016/j.neuroscience.2024.12.029
4. Hauser, S. L., andCree, B. A. C. (2020) Treatment of Multiple Sclerosis: A Review Am J Med **133**, 1380-1390.e1382 10.1016/j.amjmed.2020.05.049
5. Pukoli, D., andVecsei, L. (2023) Smouldering Lesion in MS: Microglia, Lymphocytes and Pathobiochemical Mechanisms Int J Mol Sci **24**, 10.3390/ijms241612631
6. Distefano-Gagne, F., Bitarafan, S., Lacroix, S., andGosselin, D. (2023) Roles and regulation of microglia activity in multiple sclerosis: insights from animal models Nat Rev Neurosci **24**, 397-415 10.1038/s41583-023-00709-6
7. Qin, C., Yang, S., Chen, M., Dong, M. H., Zhou, L. Q., Chu, Y. H. *et al.* (2023) Modulation of microglial metabolism facilitates regeneration in demyelination iScience **26**, 106588 10.1016/j.isci.2023.106588
8. Lloyd, A. F., andMiron, V. E. (2019) The pro-remyelination properties of microglia in the central nervous system Nat Rev Neurol **15**, 447-458 10.1038/s41582-019-0184-2
9. Kuhlmann, T., Ludwin, S., Prat, A., Antel, J., Bruck, W., andLassmann, H. (2017) An updated histological classification system for multiple sclerosis lesions Acta Neuropathol **133**, 13-24 10.1007/s00401-016-1653-y
10. Grajchen, E., Hendriks, J. J. A., andBogie, J. F. J. (2018) The physiology of foamy phagocytes in multiple sclerosis Acta Neuropathol Commun **6**, 124 10.1186/s40478-018-0628-8
11. Liu, Y., Hao, W., Letiembre, M., Walter, S., Kulanga, M., Neumann, H. *et al.* (2006) Suppression of microglial inflammatory activity by myelin phagocytosis: role of p47-PHOX-mediated generation of reactive oxygen species J Neurosci **26**, 12904-12913 10.1523/JNEUROSCI.2531-06.2006
12. Bogie, J. F. J., Grajchen, E., Wouters, E., Corrales, A. G., Dierckx, T., Vanherle, S. *et al.* (2020) Stearoyl-CoA desaturase-1 impairs the reparative properties of macrophages and microglia in the brain J Exp Med **217**, 10.1084/jem.20191660
13. O'Neill, L. A., Kishton, R. J., andRathmell, J. (2016) A guide to immunometabolism for immunologists Nat Rev Immunol **16**, 553-565 10.1038/nri.2016.70
14. Song, S., Yu, L., Hasan, M. N., Paruchuri, S. S., Mullett, S. J., Sullivan, M. L. G. *et al.* (2022) Elevated microglial oxidative phosphorylation and phagocytosis stimulate post-stroke brain remodeling and cognitive function recovery in mice Commun Biol **5**, 35 10.1038/s42003-021-02984-4

15. Leng, L., Yuan, Z., Pan, R., Su, X., Wang, H., Xue, J. *et al.* (2022) Microglial hexokinase 2 deficiency increases ATP generation through lipid metabolism leading to β-amyloid clearance Nature Metabolism **4**, 1287-1305 10.1038/s42255-022-00643-4
16. Luo, M., Liu, J., Su, Y., Jiang, T., Wu, X., Gao, P. *et al.* (2025) Regulating PPARG Reduces Lipid Accumulation in Microglia and Promotes Functional Recovery After Spinal Cord Injury Adv Sci (Weinh) **12**, e06313 10.1002/advs.202506313
17. Wculek, S. K., Heras-Murillo, I., Mastrangelo, A., Mananes, D., Galan, M., Miguel, V. *et al.* (2023) Oxidative phosphorylation selectively orchestrates tissue macrophage homeostasis Immunity **56**, 516-530 e519 10.1016/j.immuni.2023.01.011
18. Wang, L., Pavlou, S., Du, X., Bhuckory, M., Xu, H., andChen, M. (2019) Glucose transporter 1 critically controls microglial activation through facilitating glycolysis Mol Neurodegener **14**, 2 10.1186/s13024-019-0305-9
19. Norton, W. T., andPoduslo, S. E. (1973) Myelination in rat brain: changes in myelin composition during brain maturation J Neurochem **21**, 759-773 10.1111/j.1471-4159.1973.tb07520.x
20. Miron, V. E., Boyd, A., Zhao, J. W., Yuen, T. J., Ruckh, J. M., Shadrach, J. L. *et al.* (2013) M2 microglia and macrophages drive oligodendrocyte differentiation during CNS remyelination Nat Neurosci **16**, 1211-1218 10.1038/nn.3469
21. Soto-Heredero, G., Gomez de Las Heras, M. M., Gabande-Rodriguez, E., Oller, J., andMittelbrunn, M. (2020) Glycolysis - a key player in the inflammatory response FEBS J **287**, 3350-3369 10.1111/febs.15327
22. Holland, R., McIntosh, A. L., Finucane, O. M., Mela, V., Rubio-Araiz, A., Timmons, G. *et al.* (2018) Inflammatory microglia are glycolytic and iron retentive and typify the microglia in APP/PS1 mice Brain Behav Immun **68**, 183-196 10.1016/j.bbi.2017.10.017
23. Huang, Z. P., Liu, S. F., Zhuang, J. L., Li, L. Y., Li, M. M., Huang, Y. L. *et al.* (2023) Role of microglial metabolic reprogramming in Parkinson's disease Biochem Pharmacol **213**, 115619 10.1016/j.bcp.2023.115619
24. Li, J., Chen, X., Song, S., Jiang, W., Geng, T., Wang, T. *et al.* (2025) Hexokinase 2-mediated metabolic stress and inflammation burden of liver macrophages via histone lactylation in MASLD Cell Rep **44**, 115465 10.1016/j.celrep.2025.115465
25. Chen, S., Li, Q., Shi, H., Li, F., Duan, Y., andGuo, Q. (2024) New insights into the role of mitochondrial dynamics in oxidative stress-induced diseases Biomed Pharmacother **178**, 117084 10.1016/j.biopha.2024.117084
26. Loix, M., Wouters, E., Vanherle, S., Dehairs, J., McManaman, J. L., Kemps, H. *et al.* (2022) Perilipin-2 limits remyelination by preventing lipid droplet degradation Cell Mol Life Sci **79**, 515 10.1007/s00018-022-04547-0
27. Li, X., Fang, C., Li, Y., Xiong, X., Xu, X., andGu, L. (2025) Glycolytic reprogramming during microglial polarization in neurological diseases Front Immunol **16**, 1648887 10.3389/fimmu.2025.1648887

Acknowledgements – I am truly grateful for the opportunity to intern with the incredible and inspiring research team of Prof. Dr. Jerome Hendriks. This internship has significantly contributed to my experience and growth as a researcher. I would like to express my heartfelt appreciation to my supervisor, Dr. Sanne Verberk, whose guidance, support, kindness, understanding, patience, and trust have provided me with a solid foundation for my development and helped build my confidence. I sincerely mean it when I say that I couldn't have accomplished this without your support. I would also like to thank each and every team member for their support, kindness, insightful questions during our meetings, and assistance. I am also greatly moved by the support from fellow students, friends, and all members of the research team and beyond, as any progress would not be possible without this support.

Author contributions – SV designed the research and experimental set-up. SB performed all the experiments, analyzed the data, under supervision of SV. SB wrote the paper, SV gave valuable feedback and edited when necessary.

This text was supported by GenAI.

SUPPLEMENTARY INFORMATION

Table 1 – qPCR primers

Gene	Primer	Sequence
Tbp	Forward	ATGGTGTGCACAGGAGCCAAG
	Reverse	TCATAGCTACTGAACTGCTG
Cyca	Forward	GCGTCTCCTTCGAGCTGTT
	Reverse	AAGTCACCACCCTGGCA
Slc2a1	Forward	AACTGGGCAAGTCCTTTG
	Reverse	TTCTTCTTCCGCATCATC TG
Hk2	Forward	GAG CCATCCTGCAACACTTAG G
	Reverse	CAGTGCACACCTCCTTAACAATG
Nos2	Forward	GGCAGCCTGTGAGACCTTTG
	Reverse	GCATTGGAAGTGAAGCGTTTC
Il6	Forward	TGTCTATACCACTTCACAAGTCGGAG
	Reverse	GCACAACTCTTTTCTCATTTCCAC
Il1β	Forward	ACCCTGCAGCTGGAGAGTGT
	Reverse	TTGACTTCTATCTTGTTGAAGACAAACC
Tnfα	Forward	CCAGACCCTCACACTCAG
	Reverse	CACTTGGTGGTTTGCTACGAC
Cd36	Forward	GGACATTGAGATTCTTTTCCTCTG
	Reverse	GCAAAGGCATTGGCTGGAAGAAC
Plin2	Forward	GTGGAAAGGACCAAGTCTGTG
	Reverse	GACTCCAGCCGTTCATAGTTG
Abca1	Forward	CCCAGAGCAAAAAGCGACTC
	Reverse	GGTCATCATCACTTTGGTCCTTG